2013 American Control Conference (ACC)
Washington, DC, USA, June 17-19, 2013

A Computationally Efficient Thermal Model of Cylindrical Battery Cells for the Estimation of Radially Distributed Temperatures

Youngki Kim, Jason B. Siegel and Anna G. Stefanopoulou

Abstract— **This paper presents a computationally efficient thermal model of a cylindrical lithium ion battery for real-time applications. Such a model can be used for thermal management of the battery system in electrified vehicles. The thermal properties are modeled by volume averaged lumped values under the assumption of a homogeneous and isotropic volume. A polynomial approximation is then used to estimate the radial temperature distribution that arises from heat generation inside the cell during normal operation. Unlike previous control oriented models, which use discretization of the heat equation, this model formulation uses two states to represent the average value of temperature and its gradient. The model is parameterized using experimental data from a 2.3 Ah 26650 Lithium-Iron-Phosphate ($LiFePO_4$ or LFP) battery cell. Finally, a Kalman filter is applied based on the reduced order thermal model using measurements of current, voltage and surface temperature of the cell and ambient temperature. The effectiveness of the proposed approach is validated against core temperature measurements.**

I. INTRODUCTION

Over the past decades, energy storage systems utilizing lithium ion (Li-ion) batteries have become one of the most critical components for realizing efficient and clean transportation systems through electrification of vehicles, e.g., hybrid electric vehicles (HEVs), plug-in hybrid electric vehicles (PHEVs), and electric vehicles (EVs). Li-ion batteries have several advantages such as no memory effect, broad temperature range of operation, and high power discharge capability [1]. However, the Li-ion battery cycle life and capacity are adversely affected by sustained operation at high temperatures [2]. This presents a problem in automotive applications where high current rates needed for vehicle acceleration cause internal heating of the battery. Thus, being able to estimate/predict the temperature distribution across cells and packs is vital for formulating power management strategies that are mindful of the performance limitations of these versatile power/energy sources.

Physics-based thermal models are capable of accurate prediction of temperature distribution [3]. In general, numerical techniques such as finite difference method (FDM), finite element method (FEM), and finite volume method (FVM) are commonly used for solving heat or mass transfer problems in the form of partial differential equations (PDEs). However, these models are computationally intensive since a large number of ordinary differential equations (ODEs) are generated by discretizing governing equations.

Y. Kim, J. Siegel, and A. Stefanopoulou are with the Department of Mechanical Engineering, University of Michigan, Ann Arbor, MI, 48109, USA youngki@umich.edu, siegeljb@umich.edu, annastef@umich.edu

To overcome this drawback, reduced order models have been proposed using techniques such as balanced truncation method [4]. However, additional computations are required to determine which are the important modes of the system. A single or volume-averaged temperature model is used in [5]. A two-state lumped thermal model was used in [6], [7] for improved core temperature prediction with minimal increase in computational effort relative to the single state model. Nevertheless, the assumption that the heat is generated at the core of the battery cell may lead to an overestimation of the core temperature.

In this paper, we propose a computationally efficient thermal model for a cylindrical battery cell and its application for estimating core and surface temperatures. Toward this end, a polynomial is used to approximate the solution of the heat transfer problem. This approach provides a method to estimate the core and surface temperatures. The model states are the volume-averaged temperature and temperature gradient which can be directly used in the control problem formulation. Specifically, the temperature gradient can indicate the imbalance of temperature distribution inside a battery. The two-state lumped parameter model is expressed in linear state-space form that can be used in control applications for battery management systems. As a specific example, we develop a Kalman filter-based estimator for a cylindrical battery cell using the proposed model.

This paper is organized as follows. Section II presents the convective heat transfer problem for a cylindrical battery cell. The two-state thermal model using polynomial approximation is addressed. The frequency responses of the transfer function of the proposed model and analytical solution are compared to show the accuracy of the proposed model. Then, the thermal properties of the battery are experimentally identified in Section III. In Section IV, a Kalman filter-based estimator is developed using the proposed model for monitoring core temperature of the battery and the developed estimator is experimentally validated. Finally, conclusions are drawn in Section V.

II. HEAT TRANSFER PROBLEM IN CYLINDRICAL BATTERIES

This paper considers the radially distributed (1-D) thermal behavior of a cylindrical battery cell with convective heat transfer boundary condition as illustrated in Fig. 1 [8]. A cylindrical Li-ion battery, so-called a jelly-roll, is fabricated by rolling a stack of cathode/separator/anode layers. The individual layered sheets are thin, therefore, lumped parameters are used so that material properties such as

978-1-4799-0178-4/$31.00 ©2013 AACC

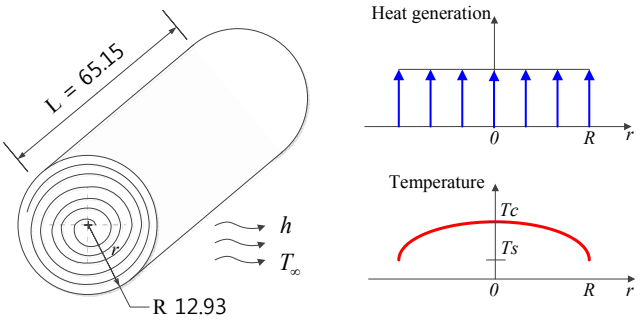

Fig. 1. Schematic for a A123 26650 cylindrical battery cell

thermal conductivity, density, and specific heat coefficient are assumed to be constant in a homogeneous and isotropic body. For spiral wound current collectors with multiple connections to the battery tab, it is reasonable to assume uniform heat generation along the radial direction [9]. The thermal conductivity is one or two orders of magnitude higher in the axial direction than in the radial direction. Therefore, the temperature distribution in the axial direction will be more uniform [10]. The governing equation of the 1-D temperature distribution $T(r,t)$ and boundary conditions are given by

$$\rho c_p \frac{\partial T(r,t)}{\partial t} = k_t \frac{\partial^2 T(r,t)}{\partial r^2} + \frac{k_t}{r}\frac{\partial T(r,t)}{\partial r} + \frac{Q(t)}{V_b}, \quad (1)$$

$$\text{B.C.'s } \frac{\partial T(r,t)}{\partial r}\Big|_{r=0} = 0, \quad (2)$$

$$\frac{\partial T(r,t)}{\partial r}\Big|_{r=R} = -\frac{h}{k_t}(T(R,t) - T_\infty), \quad (3)$$

where t, ρ, c_p and k_t represent time, volume-averaged density, specific heat coefficient, and thermal conductivity of the cell respectively. The radius of the battery cell is R, Q is the heat generation inside the cell, and V_b is the volume of battery cell. Ambient temperature for convection is denoted by T_∞. The boundary condition in (2) represent the symmetric structure of the battery about the core. The other boundary condition shown in (3) represents the convective heat transfer at the surface of the battery.

A. Model reduction

With evenly distributed heat generation, the temperature distribution along r-direction of the battery cell is assumed to satisfy the following polynomial approximation proposed in [11]

$$T(r,t) = a(t) + b(t)\left(\frac{r}{R}\right)^2 + d(t)\left(\frac{r}{R}\right)^4, \quad (4)$$

where $a(t)$, $b(t)$, and $d(t)$ are time-varying constants. To satisfy the symmetric boundary condition at the core of the battery cell, (4) contains only even powers of r. Thus, the temperatures at core and surface of the battery can be expressed as

$$T_c = a(t),\ T_s = a(t) + b(t) + d(t), \quad (5)$$

where subscripts c and s denote core and surface respectively.

The volume-averaged temperature $\bar{T}$ and temperature gradient $\bar{\gamma}$ are introduced as follows:

$$\bar{T} = \frac{2}{R^2}\int_0^R rT\,dr,\ \bar{\gamma} = \frac{2}{R^2}\int_0^R r\left(\frac{\partial T}{\partial r}\right)dr. \quad (6)$$

These volume-averaged values are used as the states unlike existing approaches in [12], [6], and [7].

By substituting (4) in (6), $\bar{T}$ and $\bar{\gamma}$ can be expressed in terms of constants as

$$\bar{T} = a(t) + \frac{b(t)}{2} + \frac{d(t)}{4},\ \bar{\gamma} = \frac{4b(t)}{3R} + \frac{8d(t)}{5R}. \quad (7)$$

By rearranging (5) and (7), time-varying constants $a(t)$, $b(t)$, and $d(t)$ can be written by

$$\begin{aligned} a(t) &= 4T_s - 3\bar{T} - \frac{15R}{8}\bar{\gamma}, \\ b(t) &= -18T_s + 18\bar{T} + \frac{15R}{2}\bar{\gamma}, \\ d(t) &= 15T_s - 15\bar{T} - \frac{45R}{8}\bar{\gamma}. \end{aligned} \quad (8)$$

By substituting (8) in (4), the temperature distribution can be expressed as a function of T_s, $\bar{T}$, and $\bar{\gamma}$

$$\begin{aligned} T(r,t) = {} & 4T_s - 3\bar{T} - \frac{15R}{8}\bar{\gamma} \\ & + \left[-18T_s + 18\bar{T} + \frac{15R}{2}\bar{\gamma}\right]\left(\frac{r}{R}\right)^2 \\ & + \left[15T_s - 15\bar{T} - \frac{45R}{8}\bar{\gamma}\right]\left(\frac{r}{R}\right)^4. \end{aligned} \quad (9)$$

The PDE (1) can be converted into ODEs by substituting (9) in volume-averaged governing equation and its partial derivative with respect to r as follows:

$$\begin{aligned} \frac{d\bar{T}}{dt} + \frac{48\alpha}{R^2}\bar{T} - \frac{48\alpha}{R^2}T_s + \frac{15\alpha}{R}\bar{\gamma} - \frac{\alpha}{k_t V_b}Q = 0, \\ \frac{d\bar{\gamma}}{dt} + \frac{320\alpha}{R^3}\bar{T} - \frac{320\alpha}{R^3}T_s + \frac{120\alpha}{R^2}\bar{\gamma} = 0, \end{aligned} \quad (10)$$

where $\alpha = k_t/\rho c_p$ is thermal diffusivity.

Using (3), the surface temperature T_s can be rewritten as

$$T_s = \frac{24k_t}{24k_t + Rh}\bar{T} + \frac{15k_t R}{48k_t + 2Rh}\bar{\gamma} + \frac{Rh}{24k_t + Rh}T_\infty.$$

Finally, a two-state thermal model can be given by the following form:

$$\begin{aligned} \dot{x} &= Ax + Bu, \\ y &= Cx + Du, \end{aligned} \quad (11)$$

where $x = [\bar{T}\ \bar{\gamma}]^T$, $u = [Q\ T_\infty]^T$ and $y = [T_c\ T_s]^T$ are states, inputs and outputs respectively. System matrices A,

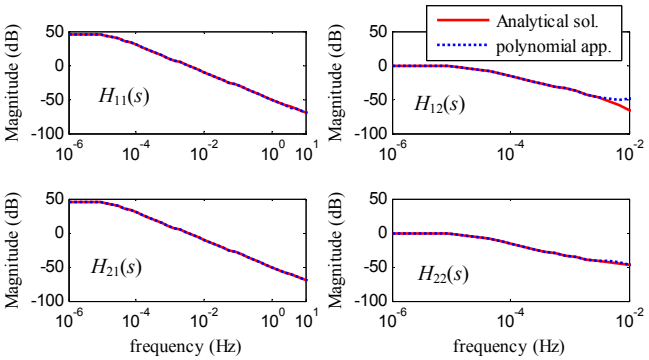

Fig. 2. Comparison of frequency response functions between analytical solution and polynomial approximation

B, C, and D are defined as follows:

$$A = \begin{bmatrix} \frac{-48\alpha h}{R(24k_t+Rh)} & \frac{-15\alpha h}{24k_t+Rh} \\ \frac{-320\alpha h}{R^2(24k_t+Rh)} & \frac{-120\alpha(4k_t+Rh)}{R^2(24k_t+Rh)} \end{bmatrix},$$

$$B = \begin{bmatrix} \frac{\alpha}{k_t V_b} & \frac{48\alpha h}{R(24k_t+Rh)} \\ 0 & \frac{320\alpha h}{R^2(24k_t+Rh)} \end{bmatrix},$$

$$C = \begin{bmatrix} \frac{24k_t-3Rh}{24k_t+Rh} & -\frac{120Rk_t+15R^2h}{8(24k_t+Rh)} \\ \frac{24k_t}{24k_t+Rh} & \frac{15Rk_t}{48k_t+2Rh} \end{bmatrix},$$

$$D = \begin{bmatrix} 0 & \frac{4Rh}{24k_t+Rh} \\ 0 & \frac{Rh}{24k_t+Rh} \end{bmatrix}. \quad (12)$$

This state-space representation is used for the parametrization in Section III and the estimation of core temperature using Kalman Filter in Section IV.

B. Frequency domain analysis

The frequency response of transfer function of the proposed model, $H(s) = D + C(sI - A)^{-1}B$, is compared to that of the analytical solution in [4]. The variable I is the identity matrix. Parameters used to generate the plots in Fig. 2 are summarized in Table I. The heat transfer coefficient of h=5W/m^{2}K is chosen since this value is typical of natural convection condition.

Figure 2 shows that the effects of heat generation on core and surface temperature, denoted by $H_{11}(s)$ and $H_{21}(s)$ respectively, can be accurately predicted over the whole range of frequency. On the other hand, the responses of core and surface temperature excited by the ambient temperature, $H_{12}(s)$ and $H_{22}(s)$, are nearly identical to the analytical solution for frequencies below 10^{-2} Hz. In general, the temperature of cooling media does not change rapidly. Thus, the prediction of temperature distribution using the proposed approach can be considered sufficiently accurate.

TABLE I
PARAMETERS OF THE BATTERY [4]

Parameter	Symbol	Value	Unit
Density	ρ	1824	kg/m^3
Specific heat coeff.	c_p	825	J/kgK
Thermal conductivity	k_t	0.488	W/mK
Convection coeff.	h	5	W/m^2-K
Radius	R	12.93e-3	m
Height	L	65.15e-3	m
Volume	V_b	3.4219e-5	m^3

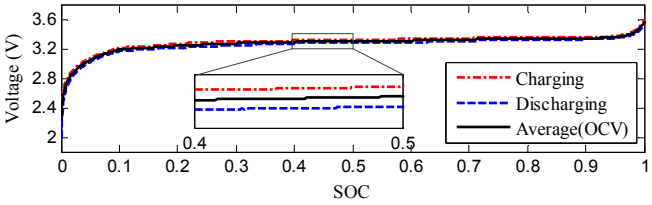

Fig. 3. Open Circuit Voltage of the 2.3 Ah 26650 LFP battery cell

C. Heat generation calculation

Since heat generation rate Q is the input to the battery thermal system, the input needs to be accurately calculated from measurement data, such as current and voltage during operation. In [5], Bernardi et al. proposed the simplified form of heat generation rate with assumptions that heat generation due to enthalpy-of-mixing, phase-change, and heat capacity are negligible as expressed by

$$Q = i(U - V) - i\left(T\frac{\partial U}{\partial T}\right), \quad (13)$$

where i, U, and V represent the current, the open-circuit voltage (OCV), and the terminal voltage respectively. As shown in Fig 3, the OCV is a function of the battery state-of-charge(SOC). This function is experimentally obtained by averaging the measured terminal voltages during charging and discharging a battery with C/20 current rate under a Constant Current Constant Voltage (CCCV) charging protocol. The OCV is then calculated at the estimated SOC value by integrating measured current with respect to time as $\dot{SOC} = -\frac{I}{3600C_b}$ where C_b is the battery capacity in Ah. The sign convention is such that positive current denotes battery discharging.

The last term in (13) is the heat generation from entropy change. In this paper, heat generation due to entropy change is neglected for simplicity. This simplification is warranted since the typical SOC range of HEV operation is narrow in which $\frac{\partial U}{\partial T}$ of the battery cell is insignificant as shown in [6] for this chemistry. In addition, the reversible entropic heat generation would have zero mean value when the battery is operating in charge-sustaining mode, typical of HEV operation.

III. PARAMETER IDENTIFICATION

In this section, the value of the lumped parameters in (11) for a 2.3 Ah 26650 LFP battery cell by A123 are identified through experimentation using the proposed model. Figure 4 shows current, voltage, calculated heat generation rate and ambient temperature profiles over the Urban-Assault Cycle (UAC) in [7] that is used for the parametrization. This cycle used for simulating military ground vehicles has significantly

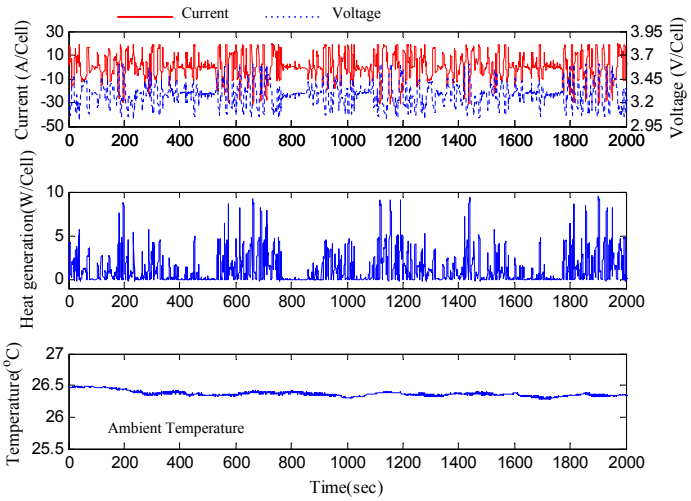

Fig. 4. Data set used for parameter ID: current and voltage (top), heat generation rate (middle), and ambient temperature (bottom) during Urban-Assault Cycle

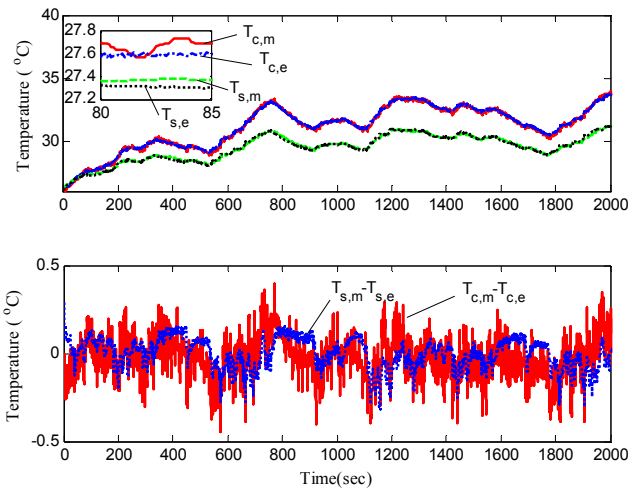

Fig. 5. Comparison between measured and simulated temperatures (top) and errors (bottom)

high power demands. The model is then validated using a different duty cycle.

A. Identifying thermal properties

Parameter identification is important for accurately predicting the temperature distribution inside a battery cell as the parameters k_t, c_p, ρ, and h determine the dynamics of thermal model. The density can be measured. Therefore, only three parameters such as k_t, c_p, and h are considered for the parameter identification. The experimental set-up is described in [7]. Measured cell current, voltage, surface and core temperatures of the battery cell, and ambient temperature are used for the parameter identification.

Let the error between the measured temperatures and model outputs at each time step k in vector form be

$$e(k,\theta) = [T_{c,e}(k,\theta)\ \ T_{s,e}(k,\theta)]^T - [T_{c,m}(k)\ \ T_{s,m}(k)]^T, \tag{14}$$

where $\theta = [k_t\, c_p\, h]^T$, $T_{c,e}$ and $T_{s,e}$ represent the model parameters, core and surface temperatures respectively. The battery is allowed to rest at ambient temperature to equilibrate, that is, $x(0) = [T_\infty\ \ 0]^T$.

Parameters are identified by minimizing the Euclidean norm of the difference between the measured and simulated temperatures as given by

$$\theta^* = arg\min_{\theta} \sum_{k=1}^{N_f} ||e(k,\theta)||_2, \tag{15}$$

where N_f is the number of measurement points. The minimization problem is solved by using the *fmincon* function in MATLAB. The parameters in Table I are used as initial guess for the identification.

TABLE II

IDENTIFIED THERMAL PROPERTIES

Parameter	Symbol	Value	Reference
Density	ρ	2047*	2118 [13]
Sp. heat coeff.	c_p	1109.2	1004.9–1102.6 [6], [7]
Thermal cond.	k_t	0.610	0.488–0.69 [4], [13]
Conv. coeff.	h	58.6	65.99 [7]

* calculated using measured mass and volume

Table II presents the identified thermal properties for the 26650 battery. These parameters are close to the values presented in the literature. The identified specific heat coefficient c_p is five percent larger than the mean value determined in [6] where c_p was determined by measuring transient responses of the battery under different pulses. Forgez et al. suggested that the deviation in identified value of c_p might be caused by measurement uncertainty in temperature and the temperature dependency of the heat capacity. The identified thermal conductivity k_t is within the range of values reported in literature [4], [13].

Despite using similar experimental data and setup, the identified convection coefficient is 11% smaller than the coefficient calculated by using thermal resistance and battery surface area in [7]. This difference may be due to the two different model structures. Lin et al. in [7] considered two different materials, namely one for the core and one for the surface, whereas we assume the battery is a homogeneous and isotropic body. To accurately determine the convection coefficient, the temperature measurements of a pure metal during thermal relaxation can be used.

Figure 5 shows the measured and simulated temperatures at the core and surface of the battery. The error between the measurements and simulated temperature is less than the sensor accuracy of 0.5^oC. Thermocouples used for temperature measurements are T-type whose accuracy is the maximum of 0.5^oC or 0.4% according to technical information from the manufacturer, OMEGA. Figure 6 shows the volume-averaged

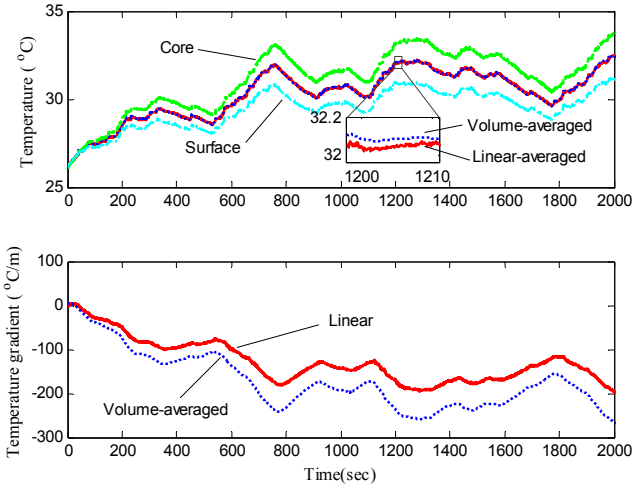

Fig. 6. Cell temperature (top) and temperature gradient (bottom)

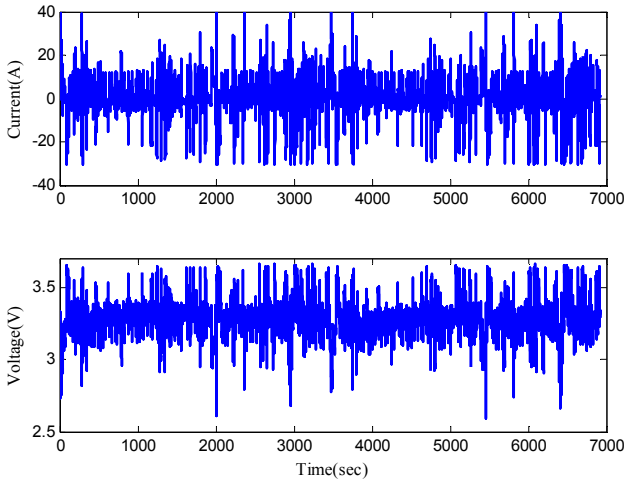

Fig. 7. Current (top) and voltage (bottom) profiles during Escort Convoy cycle

temperature and its gradient of the battery respectively. There is no significant difference between the volume-averaged temperature and the linear average of core and surface temperatures, i.e. $(T_s + T_c)/2$. Existing approaches in [6], [7] have the capability of predicting the core temperature. However, in the case of a cell with larger radius [14], the volume-averaged temperature gradient is different from the linear temperature gradient, i.e. $(T_s - T_c)/R$. In particular, the volume-averaged temperature gradient is 1.36 times greater than linear temperature gradient under the UAC test. Since non-uniform temperature distribution can lead to accelerated capacity losses of inner core [14], the volume-averaged temperature gradient is an important metric to describe severity of temperature inhomogeneity inside the battery.

B. Model validation

To validate the performance of the proposed model with the identified parameters, the battery was tested under a different HEV drive cycle, the Escort Convoy Cycle (ECC) [7]. The current and voltage profiles for this cycle are illustrated in Fig. 7. Figure 8 shows that there are slight differences between the measured and simulated temperatures; in particular, the root-mean-square errors (RMSE) of core and surface temperatures are 0.4 and 0.3^{o}C respectively. These differences may be explained with the assumption of radially uniform heat generation and high conductivity in the axial direction. Additionally, the entropy change of the LFP battery is not properly considered in heat generation formulation (13), which might introduce error in the calculation of heat generation rate. Nevertheless, since the comparison of temperatures shows good agreement and reasonably small RMSEs, it can be concluded that the proposed model with identified thermal properties is sufficiently accurate for thermal management during HEV drive cycles.

IV. TEMPERATURE ESTIMATION

In this section, we develop a Kalman filter-based (KF) estimator for monitoring the core temperature of the battery whose thermal properties were identified in previous section.

By discretizing (11), the linear discrete-time model at time step k can be obtained as follows:

$$\begin{aligned} x(k+1) &= A_d x(k) + B_d u(k), \\ y(k) &= Cx(k) + Du(k), \end{aligned} \tag{16}$$

where A_d and B_d are system matrices in discrete-time domain. Since the determinant of system matrix A in (12), $det(A) = 960\alpha^2 h/(R^3(24k_t + Rh))$, is always positive except for the case when the cell is insulated ($h = 0$), A can be considered non-singular; thus, A_d and B_d can be calculated by

$$A_d = e^{(A\Delta T)}, B_d = A^{-1}(A_d - I)B,$$

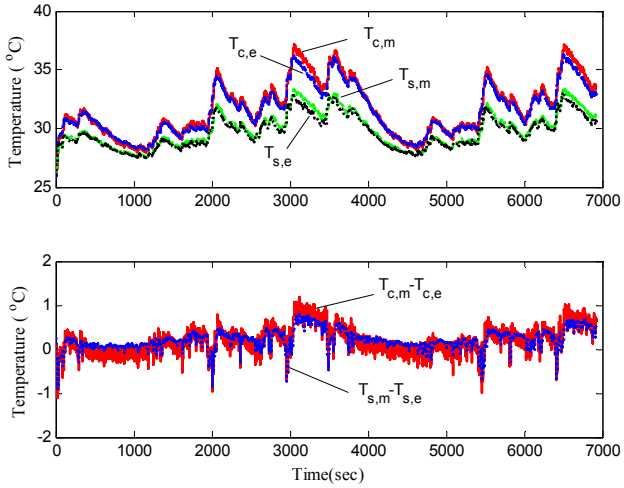

Fig. 8. Validation data set: comparison between measured and simulated temperatures (top) and errors (bottom)

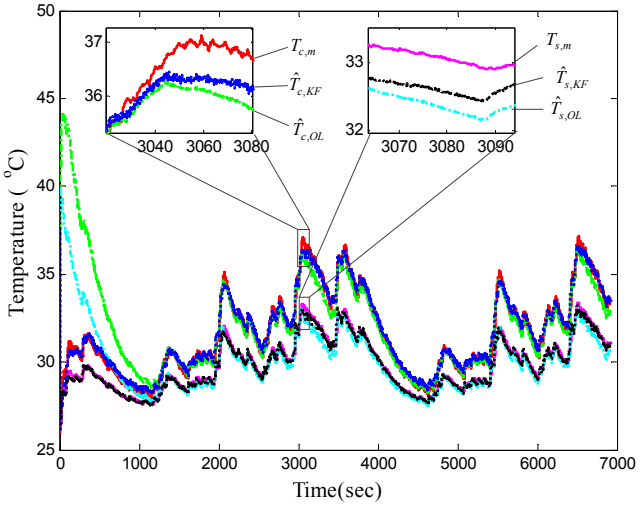

Fig. 9. Comparison of temperature estimation between Kalman Filter and open-loop prediction during ECC

where ΔT is the sampling time of 0.1 second.

The design of a KF estimator is given as following update processes.
Time update:

$$\bar{x}(k) = A_d\hat{x}(k-1) + B_d u(k-1),$$
$$\bar{P}(k) = A_d P(k) A_d^T + Q_w,$$

Measurement update:

$$K(k) = \bar{P}(k)C_2^T\left[C_2\bar{P}(k)C_2^T + R_v\right]^{-1},$$
$$P(k) = \left[I - K(k)C_2\right]\bar{P}(k),$$

where $\bar{x}$ and $\hat{x}$ are the *a priori* and *a posteriori* estimates of the state, and $\bar{P}$ and P are the *a priori* and *a posteriori* error covariances respectively. Covariance matrices Q_w and R_v are determined by zero-mean Gaussian noise in process and measurement respectively. The subscript 2 denotes elements in the second row relating to surface temperature T_s, which is the measurable output.

We assume that initial temperature distribution inside the battery is uniform at 40^oC, i.e. $\hat{x}(0) = [40\ 0]^T$. The actual temperature is 26^oC. The covariance matrix $Q_w = \beta^2\text{diag}(1,1)$ describes the process noise where β>0 is a parameter for tuning based on model inaccuracy. The noise covariance $R_v = \sigma^2$ is determined from the standard deviation of temperature signal $\sigma = 0.05^o$C. Ultimately, the initial condition of the error covariance matrix and the tuning parameter are chosen as $P(0) = \text{diag}(1,1)$ and $\beta = 0.0005$ through repeated simulations. As seen from Fig. 9, the core temperature can be accurately estimated using the KF estimator. In particular, the RMSEs of core temperatures by the KF estimator and open-loop prediction are 0.2 and 2.1 ^{o}C respectively.

V. CONCLUSION

In this study, a radially distributed 1-D thermal modeling approach for a cylindrical battery cell is proposed. Polynomial approximation is applied to obtain a reduced order model. Frequency domain analysis shows that the proposed model provides sufficiently accurate prediction of core and surface temperatures with a reasonable assumption that the temperature of cooling media does not change rapidly.

The proposed model is used to identify thermal properties and convective coefficient for a 2.3 Ah 26650 LFP battery cell using a set of measured data: current, voltage, temperature at core, surface and ambient temperatures over the UAC test. The identified parameters are close to the values in literature. The proposed thermal model can accurately predict core, surface, volume-averaged temperature, and volume-averaged temperature gradient of a cylindrical Li-ion battery. Particularly, the volume-averaged temperature gradient captures the imbalance of temperature distribution which is useful for controlling battery cooling system.

The identified properties are then used to estimate battery core temperature by applying Kalman filtering theory during a different vehicle drive cycle, the ECC. The results shows that the core temperature can be accurately estimated by using the proposed model with measured current, voltage, surface and ambient temperature which are relatively easy to measure in practice.

REFERENCES

[1] R. Huggins, *Advanced Batteries: Materials Science Aspects, first edition*. Springer, 2008.

[2] G. M. Ehrlich, "Lithium-ion batteries," in *Handbook of Batteries, third edition*, ch. 35, McGraw-Hill, 2002.

[3] C. Y. Wang and V. Srinivasan, "Computational battery dynamics (cbd)-electrochemical/thermal coupled modeling and multi-scale modeling," *Journal of Power Sources*, vol. 110, pp. 364–376, August 2002.

[4] M. Muratori, N. Ma, M. Canova, and Y. Guezennec, "A model order reduction method for the temperature estimation in a cylindrical li-ion battery cell," vol. 1, pp. 633–640, 2010.

[5] D. Bernardi, E. Pawlikowski, and J. Newman, "General energy balance for battery systems.," *Journal of the Electrochemical Society*, vol. 132, no. 1, pp. 5 – 12, 1985.

[6] C. Forgez, D. Vinh Do, G. Friedrich, M. Morcrette, and C. Delacourt, "Thermal modeling of a cylindrical lifepo4/graphite lithium-ion battery," *Journal of Power Sources*, vol. 195, no. 9, pp. 2961 – 2968, 2010.

[7] X. Lin, H. E. Perez, J. B. Siegel, A. G. Stefanopoulou, Y. Li, R. D. Anderson, Y. Ding, and M. P. Castanier, "Online parameterization of lumped thermal dynamics in cylindrical lithium ion batteries for core temperature estimation and health monitoring," *IEEE Transactions on Control System Technology, in press*, 2013.

[8] S. A. Hallaj, H. Maleki, J. Hong, and J. Selman, "Thermal modeling and design considerations of lithium-ion batteries," *Journal of Power Sources*, vol. 83, no. 1-2, pp. 1–8, 1999.

[9] D. H. Jeon and S. M. Baek, "Thermal modeling of cylindrical lithium ion battery during discharge cycle," *Energy Conversion and Management*, vol. 52, no. 8-9, pp. 2973–2981, 2011.

[10] H. Maleki, S. A. Hallaj, J. R. Selman, R. B. Dinwiddie, and H. Wang, "Thermal properties of lithium-ion battery and components," *Journal of The Electrochemical Society*, vol. 146, no. 3, pp. 947–954, 1999.

[11] V. R. Subramanian, V. D. Diwakar, and D. Tapriyal, "Efficient macro-micro scale coupled modeling of batteries," *Journal of the Electrochemical Society*, vol. 152, no. 10, pp. A2002 – A2008, 2005.

[12] C. W. Park and A. K. Jaura, "Dynamic thermal model of li-ion battery for predictive behavior in hybrid and fuel cell vehicles," in *SAE World Congress 2003-01-2286*, 04 2003.

[13] H. Khasawneh, J. Neal, M. Canova, Y. Guezennec, R. Wayne, J. Taylor, M. Smalc, and J. Norley, "Analysis of heat-spreading thermal management solutions for lithium-ion batteries," *ASME Conference Proceedings*, vol. 2011, no. 54907, pp. 421–428, 2011.

[14] K. Smith, G.-H. Kim, and A. Pesaran, "Modeling of nonuniform degradation in large-format li-ion batteries," in *215th Electrochemical society meeting, May 25 - 29*, 2009.